

Electron Transport in the Assemblies of Multiwall Carbon Nanotubes

Vladimir Samuilov, Jean Galibert and Nikolai Poklonski

Abstract

The assemblies (films) of carbon nanotubes (CNTs) possess very stable, reproducible, and extraordinary electronic properties. These films have been considered as attractive materials for various nanosensors and as electrodes of electrochemical energy storage devices, like supercapacitors, with low equivalent series resistance and highly developed internal surface. In order to develop CNT devices operating at the room temperature, it was necessary to determine the assembled films' properties, such as the mechanism of conductivity, carrier concentration, and mobility. In this study, we are focused on the assemblies (monolayers, arrays, and films) of multiwall carbon nanotubes (MWCNT). We applied a wide temperature range resistance and magnetoresistance as a tool to determine the transport characteristics of MWCNT films. The measurements of the electrical transport (temperature dependence of the resistance) in the assemblies of nanotubes were tested in the temperature range $T = 1.5\text{--}300\text{ K}$, and the magnetoresistance measurements were carried out in pulsed magnetic fields up to 35 tesla in the temperature range 1.5–300 K. The mechanisms responsible for the transport in these systems, including weak localization, antilocalization, Luttinger liquid, Shubnikov–de Haas oscillations, and intertube coupling, were observed.

Keywords: films of carbon nanotubes, MWCNT, temperature dependence of resistance, magnetoresistance, localization

1. Introduction

Since their discovery [1], carbon nanotubes revealed remarkable properties, which made them as an attractive material in broad domain of applications [2–4]. In carbon nanotube electronics [5, 6], they were expected to be used as the components of nanostructured field effect transistors [5, 7–9]. Their high anisotropic shape is considered to be useful for low field emission displays. Carbon nanotubes exhibited unique mechanical properties. Their huge elastic modulus ($\sim 1\text{ TPa}$) [10, 11] and their large surface area per volume made them good candidates, respectively, for composite materials [12] and lithium ion storage [13], for sustainable energy supplies, and for gas [14], chemical [15, 16], and bio- [17–21] sensors.

The electrical transport properties are the most important for a number of applications of carbon nanotubes. Usually, single-tube samples are used for electrical transport studies. The kinetic inductance of individual nanotubes contributes to

the low-frequency impedance of fibers composed of SWCNTs (at cryogenic temperatures and a constant electric bias) [22, 23]. Quantum transport properties have been observed both in single-wall (SWCNT) [5, 9, 24–29] and multiwall nanotubes (MWCNT) [3, 30–35].

Quantum interference effects, such as weak localization (WL), the Aharonov–Bohm (AB) effect, the Al'tshuler–Aronov–Spivak (AAS) effect, and universal conductance fluctuations (UCF), have previously been observed in multiwalled carbon nanotubes [32]. Knowledge of phase-breaking effects in coherent transport is very important for the study of these quantum interference phenomena. The temperature (T) dependence of the phase coherence length, L_ϕ , of MWCNTs has been reported to follow a power law dependence of $T^{-1/3}$, a characteristic of one-dimensional interference [36]. In the case of single-walled CNTs, the power law dependence also shows a $T^{-1/3}$ dependence [28]. In addition, as further evidence of low-dimensional transport, there are some experimental reports of Tomonaga–Luttinger liquid behavior in CNTs [37].

From one point of view, for the array (assemblies) of nanotube samples, the synergetic properties were expected only [38]. But, the transport in the arrays of nanotubes was found to show single nanotube properties at low temperatures due to the mostly conductive nanotubes responsible for the transport [25]. On the other hand, for specific new applications, like chemical [15, 16] and bio- [17–21] sensors, the synergetic properties of the arrays of nanotube samples are important [39]. They are based on their large surface area per volume and intertube coupling in electrical transport in the arrays of nanotubes [40].

The examples of different morphologies of the samples of arrays of nanotubes involve definitions of bundles (ropes) [32, 38, 41–43], mats [44, 45], networks [46, 47], and films [48]. Some of them were manufactured using hardly controlled deposition from an organic solvent dispersion of pristine nanotubes [49].

The Langmuir–Blodgett (LB) technique was found to be a method for depositing defect-free, molecularly ordered ultrathin films with controlled thickness and orientation. Since pristine nanotubes are non-soluble in many kinds of organic solvents, it is impossible to form LB films directly from nanotubes. The LB monolayer of SWCNTs by dispersing them in a surfactant was obtained on a solid substrate in [50–52]. However, due to their limited dispersibility, the concentration of nanotubes in the layer was quite low (<7%), and the control of the tube orientation was not achieved by this method. The LB film of SWCNTs grafted by polyethylene oxide (PEO) was realized [53]. However, due to the soft PEO film covering the top surface of SWCNT cores, the low collapse pressure (~15 mN/m) was achieved. It became clear that, for the formation of a monolayer of carbon nanotubes using the LB technique, chemical modification of nanotubes is required.

The organic functionalization of carbon nanotubes has been realized [54–56]. But, to our knowledge, there was no experimental data on electrical and magneto-transport properties' characterization of dense monolayers manufactured using LB assembling of functionalized nanotubes. This method is expected to be used for obtaining the layers of very dense arrays of nanotubes for using them for new applications in chemical and biosensors, controlled by electrical transport.

We utilized assembly of different carbon nanotubes in the layers:

- Pristine (non-modified) CNTs.
- Modified by organic chemical functionalization.
- Oxidized CNTs in the solution of sulfuric and nitric acids.

We describe the methods of modification and assembly of CNTs and the specificity of the electrical transport in the layers in respect to the technological approach utilized.

2. Pristine MWCNT (no modification/functionalization)

The purified MWCNTs were dissolved in chloroform/chlorobenzene mixture with the concentration up to 10^{-2} mg/ml of visually non-scattered solution after sonication. A droplet of this solution was spread on the water surface, and after evaporation of the solvent, an array of MWCNT was collected on the substrate with in-plane macroscopic finger-shaped electrodes. The resistance was measured as a function of temperature and magnetic field in the Laboratoire National des Champs Magnetiques Intenses de Toulouse in the range 1.8–300 K and up to 35 T. We review here the most typical features of our results obtained on these non-functionalized self-assembled arrays of MWCNT.

Between 4.2 and 70 K, the zero magnetic field resistance (**Figure 1**) exhibited a behavior as $R \propto R_0 + AT^{-\alpha}$, where $\alpha = 0.38$, while in the range 60–300 K, the resistance behaved like $R \propto R_0' + BT^{-1/3}$.

As a power law can fit the temperature dependence of the resistance, the formation of a Luttinger liquid in which the transport is managed by coherent backscattering effects could be suggested [35]. Similar power law temperature dependence with the same exponent was found earlier in SWCNT samples [25, 26].

With the magnetic field B perpendicular to the plane of our sample, a negative magnetoresistance (NMR) is observed in the whole range of magnetic fields and in the temperatures between 1.8 and 80 K, with a tendency to a saturation at high magnetic fields.

Also, the magnetoresistance shows some oscillations in the magnetic field up to 30 T, at 1.8 K, as it can be seen in **Figure 2**. At higher temperatures these oscillations tend to vanish. The oscillations can be attributed to the Shubnikov–de Haas (SdH) oscillations. They are clearly seen without background subtraction.

A maximum occurs in the resistance at magnetic field B_n when the Fermi energy E_F crosses a quantized energy level E_n in the field. In graphene [57],

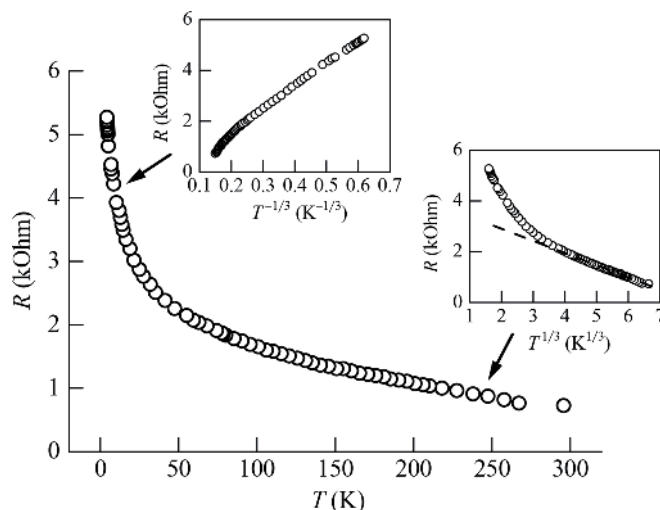
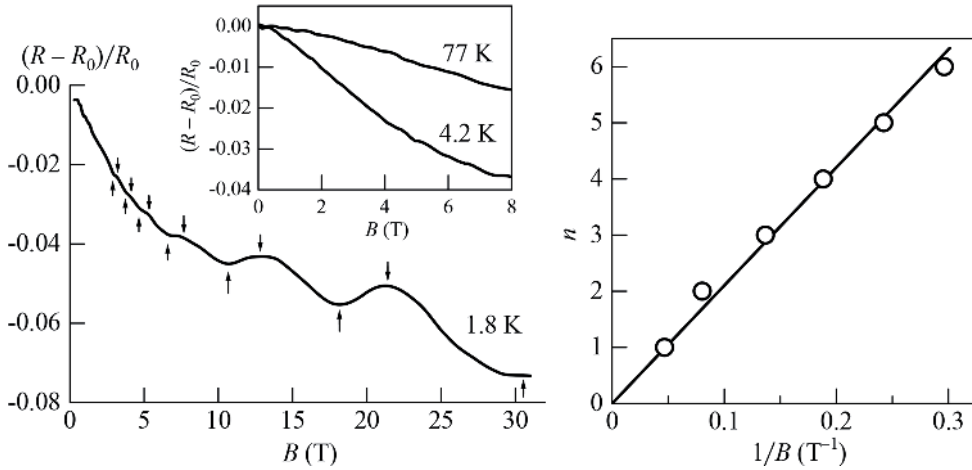


Figure 1. Temperature dependence of the resistance of an array of pristine MWCNT sample. In the insets, the dependence $R(T)$ is shown in the low and high temperature range.


Figure 2.

Transverse magnetoresistance at 1.8 K shows some oscillations in the magnetic field up to 30 T. In the inset the magnetoresistance dependences at $T = 4.2$ K and at $T = 77$ K show no significant oscillations. The maxima of resistance oscillations are labeled with n and plotted as a function of $1/B_n$ in a Landau plot in the second inset.

$E_n(B) = \sqrt{(2n_e B v_0^2)}$ [58] and $B_n = B_0/n$, where $B_0 = E_F^2/(2ev_0\hbar^2) = \hbar k_F^2/2e$. Each maximum is labeled with n and plotted as a function of $1/B_n$ in a Landau plot (inset of **Figure 2**). The well-identified peaks ($n = 1-6$) define a straight line. From the slope we determine k_F and $n_s = 4k_F^2/4\pi \approx 1.9 \times 10^{12} \text{ cm}^{-2}$, which is consistent with the experiment [59].

At this stage of our investigation in these samples, we intend to suggest some explanation of the behavior of the NMR. The transverse NMR has been observed at low magnetic field with a superposition of some aperiodic oscillations consistent with the universal conductance fluctuations (UCF) [3, 30]. From a classical point of view, the interference term leading to UCF originates from adding the probability amplitudes of all paths that connect the source and drain. The NMR at low field is caused by interference contributions due to closed electron trajectories, which add up constructively at zero magnetic field; that could be considered as the definition of WL [60]. A correct treatment would need the use of the digamma functions [61, 62].

While WL is expected to decay slower with the temperature than UCF, a study of the NMR at different temperatures will allow us to discriminate from these two processes. If not, it will signify that the fluctuations could be due to the band structure of the ensemble of nanotubes and might be caused by magnetic depopulation of a one-dimensional sub-band, a phenomenon which, in extended thin films, gives rise to SdH oscillations [60].

It must be noticed that the MWCNT in our samples were not arranged as a film but rather form a “carpet” which, under some conditions, should be considered as a 2DEG. In the MWCNT films, the NMR was observed also at low magnetic fields [48], followed by a positive magnetoresistance (PMR), till 12 T. It was argued that the NMR may come from (i) quantum interference [63, 64], (ii) thermal fluctuation-induced tunneling [65], or (iii) Landau levels in disordered graphite [66]. In our case, as the NMR was observed till 25 T and at low temperature, the hypotheses (i) and (ii) can be rejected. As far as the Landau levels, or SdH oscillations [3], could be considered, we notice that the oscillations observed in our experiments appear to be mainly periodic in $1/B$ (in contradiction with which was observed in [3, 30]) and might be related to the SdH oscillations.

As a result, in this section, we report the experiments on temperature and magnetic field dependence of the resistance of self-assembled assemblies of pristine

MWCNT, in which we attribute the NMR in terms of WL and interpreted the oscillations in terms of SdH behavior.

3. Chemically functionalized multiwall carbon nanotubes

The electrical transport properties are the most important for a number of applications of carbon nanotubes. Usually, single-tube samples are used for electrical transport studies. Quantum transport properties have been obtained both in single-wall (SWCNT) [5, 9, 24–28] and multiwall nanotubes (MWCNT) [3, 30–35]. For the nanotube array samples, only mean values of the characteristic parameters were expected [38]. But, in some cases, the transport in the arrays of nanotubes was found to show single nanotube properties at low temperatures due to the mostly conductive nanotubes responsible for the transport [25]. On the other hand, for the specific applications, like chemical [15, 16] and bio- [17–21] sensors, the synergetic properties of the arrays of nanotube samples are important. They are based on their large surface area per volume and intertube coupling in electrical transport in the arrays of nanotubes [40].

We have shown experimentally that chemically functionalized multiwall carbon nanotubes could be assembled into 2D layers (dense arrays) covering large surfaces with in-plane electrodes for electrical and magnetotransport testing.

In contrast to the standard morphologies of the samples of arrays of nanotubes involving definitions of bundles (ropes), mats, networks, etc., based on hardly controlled deposition from an organic solvent dispersion of pristine nanotubes, we use the LB technique for chemically functionalized multiwall carbon nanotubes. The method we propose offers a radical departure from the existing methodology due to the possibility of covering large surfaces with dense and defect-free, molecularly thin films of carbon nanotubes.

The electrical and magnetotransport properties in the assembled monolayers of carbon nanotubes have been tested.

The organic functionalization of carbon nanotubes had been realized [54–56, 67–69]. But, to our knowledge, up to now, the experimental data on electrical and magnetotransport properties' characterization of dense monolayers manufactured using LB assembling of functionalized nanotubes is very limited. This method is expected to be used for obtaining the layers of very dense arrays of nanotubes for utilizing them for new applications in chemical and biosensors, controlled by electrical transport.

The MWCNTs produced by chemical vapor decomposition (CVD) with catalyst 5% Fe-Co/CaCO₃ were utilized.

Organic functionalization of MWCNTs was based on the scheme described in [69].

The purified MWCNTs were suspended in N,N-dimethylformamide [DMF] HCON(CH₃)₂ together with excess *p*-anisaldehyde (4-methoxybenzaldehyde) CH₃OC₆H₄CHO and 3-methylhippuric acid [m-toluric acid, N-(3-methyl-benzoyl) glycine] CH₃C₆H₄CONHCH₂CO₂H.

Heterogeneous mixture was heated at 130°C for 3 days. The scheme of the reaction is described in **Figure 3**. After the reaction was stopped, the organic phase was separated from unreacted material by centrifugation and washing five times with chloroform (CHCl₃) and vacuum drying. The obtained dark solid phase was easily soluble in CHCl₃ up to a few mg/ml without sonication. The functionalized nanotubes were tested by HRTEM (**Figure 4**) and FTIR (**Figure 5**) methods. Due to the distinct layer on the surface of the nanotubes, observed by HRTEM (**Figure 4**), which is responsible for the absorption peaks in 1400–1500 cm⁻¹ and 1800–1900 cm⁻¹ on FTIR spectra (**Figures 5 and 6**), we conclude that the

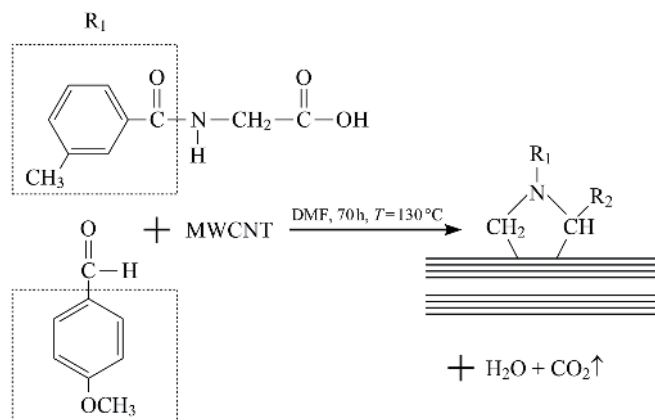


Figure 3. The scheme of the reaction of organic functionalization of MWCNTs. The purified MWCNTs were suspended in *N,N*-dimethylformamide [DMF] $\text{HCON}(\text{CH}_3)_2$ together with excess *p*-anisaldehyde (4-methoxybenzaldehyde) $\text{CH}_3\text{OC}_6\text{H}_4\text{CHO}$ and 3-methylhippuric acid [*m*-toluric acid, *N*-(3-methyl-benzoyl) glycine] $\text{CH}_3\text{C}_6\text{H}_4\text{CONHCH}_2\text{CO}_2\text{H}$. Heterogeneous mixture was heated at 130°C for 3 days.

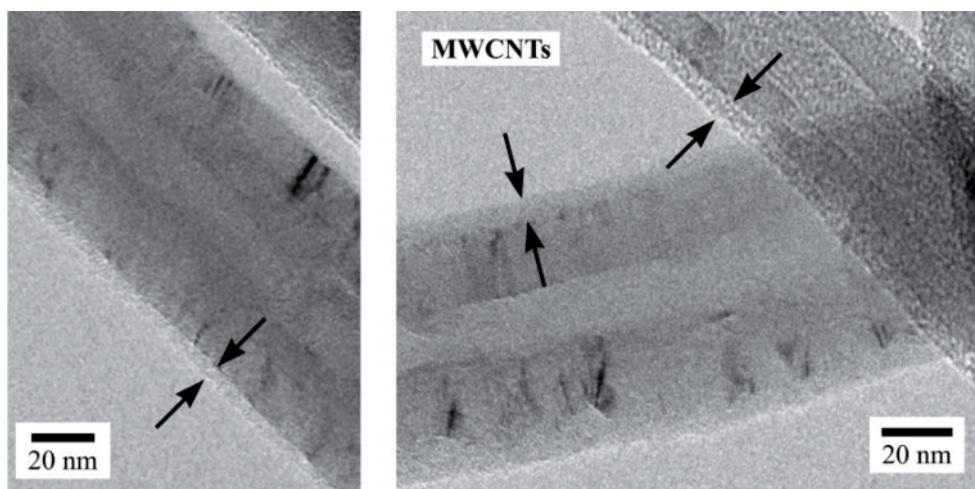


Figure 4. High-resolution TEM image of organically functionalized MWCNT. The nanotubes are covered with the thin organic layer (shown with the arrows).

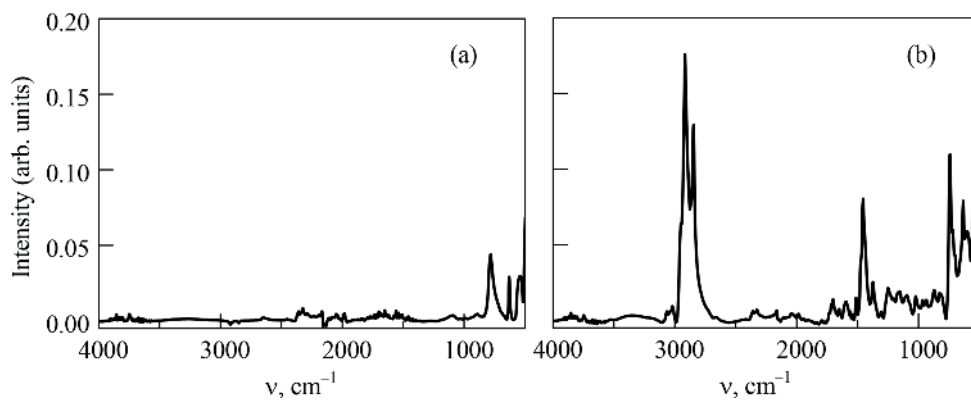


Figure 5. FTIR spectra of MWCNTs: no functionalization (a); with functionalization (b).

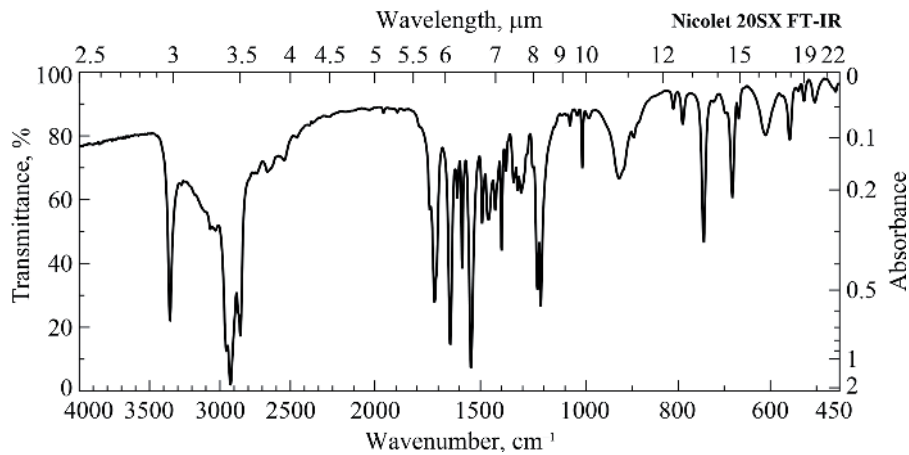


Figure 6. FTIR spectrum 3-methylhippuric acid, condensed phase. Adapted from the Sigma-Aldrich catalog: <https://www.sigmaaldrich.com/spectra/ftir/FTIR005396.PDF>.



Figure 7. Functionalized nanotubes self-assembled in dense arrays (monolayers), covering without empty space the whole surfaces of the finger-shaped electrode device.

functionalization procedure described in [69] for single-wall carbon nanotubes works for MWCNTs. An important feature of FTIR spectrum of MWCNT is the absence of -COOH group peak near 3350 cm^{-1} . This fact has proven covalent bonding of 3-methylhippuric acid and *p*-anisaldehyde with MWCNTs, and not just physical adsorption of the surfactant.

The deposition of the layers (arrays) of nanotubes on the surface of the devices with the electrodes was done by using the cell, imitating the LB trough. Once a droplet of the solution of functionalized nanotubes in chloroform was spread on the water surface, a droplet of diblock copolymer PS-PMMA solution was added in order to create surface pressure of $\sim 9\text{ mN/m}$. Functionalized nanotubes were self-assembled in dense arrays (monolayers), covering without empty space the whole surfaces of the finger-shaped electrode devices, when the monolayer was picked up from the water surface (**Figure 7**). The same layer of MWCNTs on the substrate at higher magnification with SEM is shown in **Figure 8**.

Utilizing LB method for functionalized nanotubes has shown reliable and reproducible *p*-*A* isotherms. Based on this, we expect to use LB method for covering large surfaces with dense and defect-free, molecularly ordered ultrathin films of carbon nanotubes with controlled thickness and orientation.

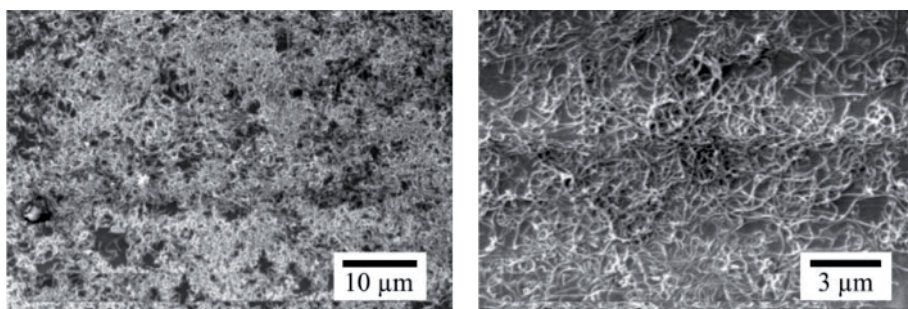


Figure 8. SEM images of the dense arrays (monolayers) of functionalized MWCNTs, covering surfaces of the substrate.

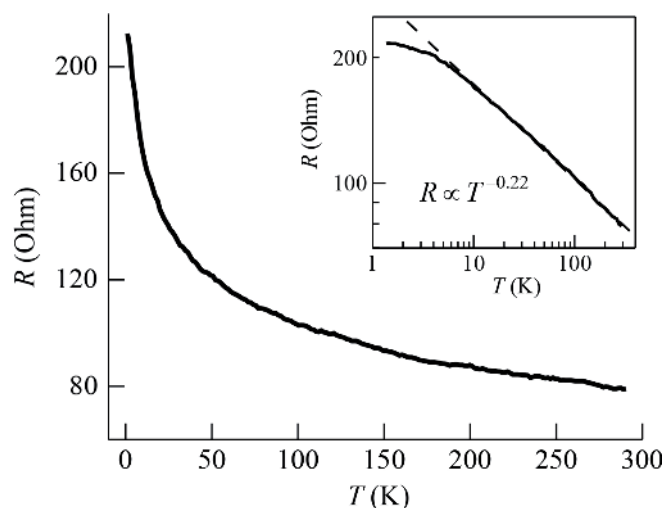


Figure 9. The temperature dependence of the resistance of the functionalized MWCNT sample. In the inset, dependence is the same in the $\log R$ vs. $\log T$ scale. The linear dependence in the double log scale in the range 10–300 K gives a power law with an exponent -0.22 for the temperature dependence.

The electrical and magnetotransport properties of the layers (arrays) of multi-wall carbon nanotubes have been tested in the temperature range 1.8–300 K and in magnetic fields up to 35 T.

The nanotube samples on the electrodes with “finger-shape” geometry (**Figure 7**) have shown low resistance (<1 kOhm at room temperature) and a “weak” temperature dependence of the resistance in the shape of power law in the temperature range $T = 4.2$ –300 K.

The temperature dependences of the resistance in linear and log–log scales for arrays of the functionalized nanotubes are presented in **Figure 9**. It is interesting to point out that the temperature dependences of the resistance are represented by the power law with the exponent -0.22 . While a power law can fit the temperature dependence of the resistance in MWCNT, a behavior suggestive of the formation of a Luttinger liquid, in which the transport is managed by coherent backscattering effects, can be considered [35]. Similar power law temperature dependence with the same value of the exponent was found earlier in SWCNT “bundle” samples deposited on the top of the contacting electrodes [25, 26].

The saturation at low temperatures is noticeable on $R(T)$ dependence of functionalized nanotubes. This could be explained in the framework of Coulomb blockade and tunneling between tubes through thin organic layers, covering MWCNT surfaces.

The magnetoresistance measurements were carried out in pulsed magnetic fields up to 35 T in the temperature range 1.8–80 K (**Figure 10**). The magnetic field

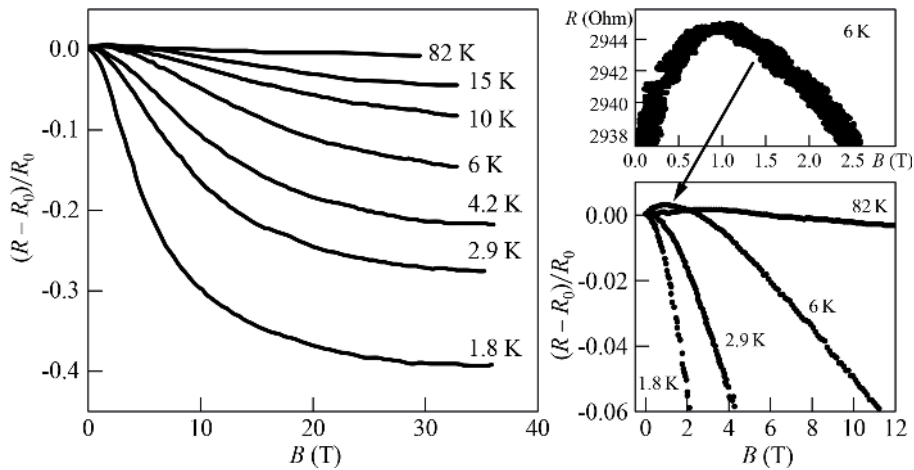


Figure 10.
The magnetoresistance of the functionalized MWCNT sample is carried out in pulsed magnetic fields up to 35 T in the temperature range 1.8–80 K.

orientation in relation to the current direction was considered “normal” to the current direction.

With the magnetic field B perpendicular to the plane of the sample, NMR was observed in the whole range of available magnetic fields between 1.8 and 80 K in the arrays of functionalized nanotubes (Figure 10). As already reported in section 2, the NMR was believed to be observed due to the interference contributions of the closed electron trajectories, which add up constructively at zero magnetic field; that could be considered as the definition of WL [60]. A correct treatment should be based on the use of the digamma function [61, 62].

In addition to the NMR at high fields for functionalized nanotubes, we can see a positive magnetoresistance at low fields (inset in Figure 10). The positive magnetoresistance increases quadratically and saturates at fields above $B = 2$ T. The weak antilocalization effect [70–72] in multiwall carbon nanotubes [73] appears to be responsible for the positive magnetoresistance. It is attributed to the spin-dephasing process, arising from the local interfacial fields as a genuine property of the curved multiwall tubes [73].

We have reported the experimental observation of the electrical transport properties of assembled (layers) arrays of non-functionalized and functionalized MWCNTs. The negative magnetoresistance as a characteristic of weak localization state was observed. In addition to the negative magnetoresistance at high fields for functionalized nanotubes, we observed positive magnetoresistance at low fields.

4. Oxidized carbon nanotubes

This technology introduces the formation of oxidized multiwalled carbon nanotubes. Oxidized MWCNTs become hydrophilic and soluble in water. In order to assemble uniform monolayers of MWCNTs on large surfaces we have developed, the so-called “inverted” Langmuir–Blodgett technique, the essence of which is clear from Figure 11. The method consists of the following major technology steps. MWCNT oxidation can be carried out by means of oxidizing liquids such as sulfuric and nitric acids.

MWCNT is dispersed in acid solution (3:1 = H_2SO_4 : HNO_3) and ultra-sonicated for a few hours in a water bath at the elevated temperatures. The solution was stirred

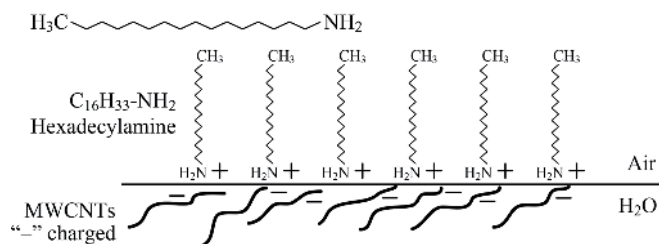


Figure 11. Schematics of the inverted Langmuir-Blodgett technique for the monolayers of MWCNT assembly.

very well simultaneously. The mixture is filtered by using 0.1-micron polyvinylidene fluoride (PVDF) filter. The filtered oxidized MWCNT is extensively washed with distilled water until pH became neutral. The powder was dried in the oven.

This method generates oxygenated functional groups (-OH, -C=O, and -COOH).

Hydroxyl (-OH) groups are not highly reactive, but they readily form hydrogen bonds and contribute to making molecules soluble in water.

Carbonyl (-C=O) groups have one oxygen atom double-bonded to a carbon atom (symbolized as C=O). Like hydroxyl groups, carbonyl groups contribute to making CNTs water-soluble.

The carboxyl group (symbolized as -COOH) has both a carbonyl and a hydroxyl group attached to the same carbon atom, resulting in new properties—it can be ionized—releasing the H from the hydroxyl group as a free proton (H^+), with the remaining O carrying a negative charge.

MWCNT monolayers were prepared by dispersion in deionized water at the concentration of 0.04–0.05 mg/ml. The surfactant hexadecylamine is dissolved in chloroform to prepare the spreading solution at the concentration of 1 mg/ml and spread onto the surface of the oxidized MWCNT solution in the LB trough. The floating monolayer of highly polarized surfactant molecule, having positively charged hydrophilic ends, makes monolayers with negatively charged oxidized carbon nanotubes through electrostatic interaction. The hybrid monolayer compressed in the LB trough at a rate of a few mm/min. Surface pressure-area (p-A) isotherm

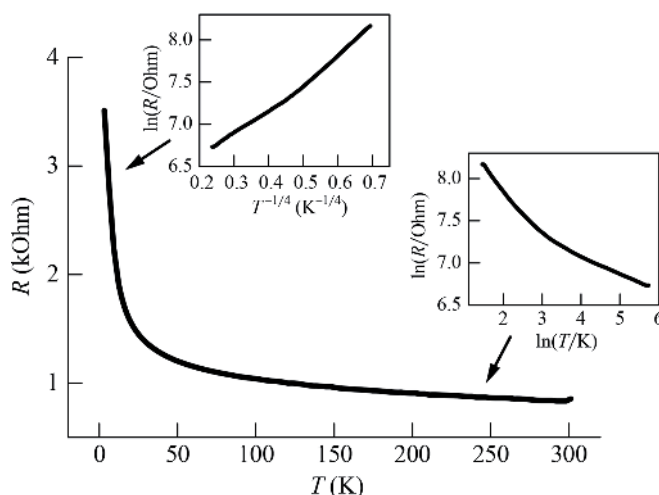


Figure 12. The temperature dependence of the resistance of the oxidized MWCNT sample. In the insets, low temperature range dependence in the $\ln R$ vs. $T^{-1/4}$ scale shows localization regime of conductivity. The linear dependence in the double \ln scale high temperature range gives a power law temperature dependence.

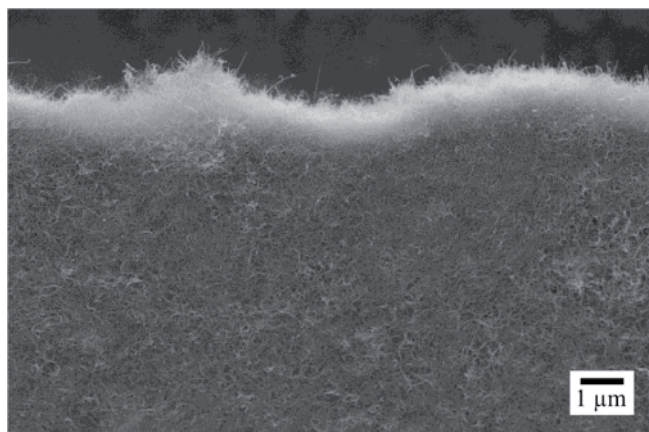


Figure 13.
SEM image of a few micrometer-thick oxidized MWCNT membrane.

curves of the hybrid monolayers are recorded during the compression. The hybrid monolayers were deposited by vertical dipping on a clean hydrophilic surface. After deposition, the surface of the transferred film was dried in a flow of N_2 gas.

The electrical transport properties of the monolayers (arrays) of the oxidized multiwall carbon nanotubes have been tested in the temperature range 4.2–300 K and represented in **Figure 12**.

The oxidized MWCNTs can be assembled in the freestanding layers of arbitrary thickness, utilizing vacuum filtering technique. The resulting MWCNT membranes are very stable and can be further utilized for sensor and energy storage applications. **Figure 13** shows the SEM image of a few micrometer-thick membrane.

5. Nano-catalysis

The common catalysis-oriented goals are to understand and predict the properties of nanosized materials and control how they facilitate chemical reactivity. Another critically important issue deals with the manufacture of nanoscale components from the bottom up and finally to integrate nanoscale components into macroscopic scale objects and catalysts for real-world uses.

We have shown a very strong catalytic activity of an outer surface of MWCNT, modified by acid oxidation. Nanocrystals of NaF were formed on the surface of MWCNT (**Figure 14**). We have also observed metal nanocrystal “decoration” on the surface of MWCNTs.

For example, electrolytic water splitting represents the most environmentally friendly alternative to generate hydrogen gas. However, the kinetics of the oxygen evolution reaction (OER) are slow and require a catalyst. Most catalysts to date have been limited to transition metal oxides or noble metals—both of which are expensive and unsustainable. The OER activity rationalized by the oxygen-containing functional groups on the surface of oxidized MWCNTs alters the electronic distribution of the surrounding carbon atoms at the MWCNT surfaces, thereby facilitating the adsorption of water oxidation intermediates. This opens the door to new applications of surface-oxidized MWCNTs for catalyzing a class of important anodic reactions in water splitting and fuel cells. Further improvements of the activity of the surface-oxidized carbon nanomaterials may enable the fine-tuning of the structure and compositions of hybrid carbon materials for specific applications.

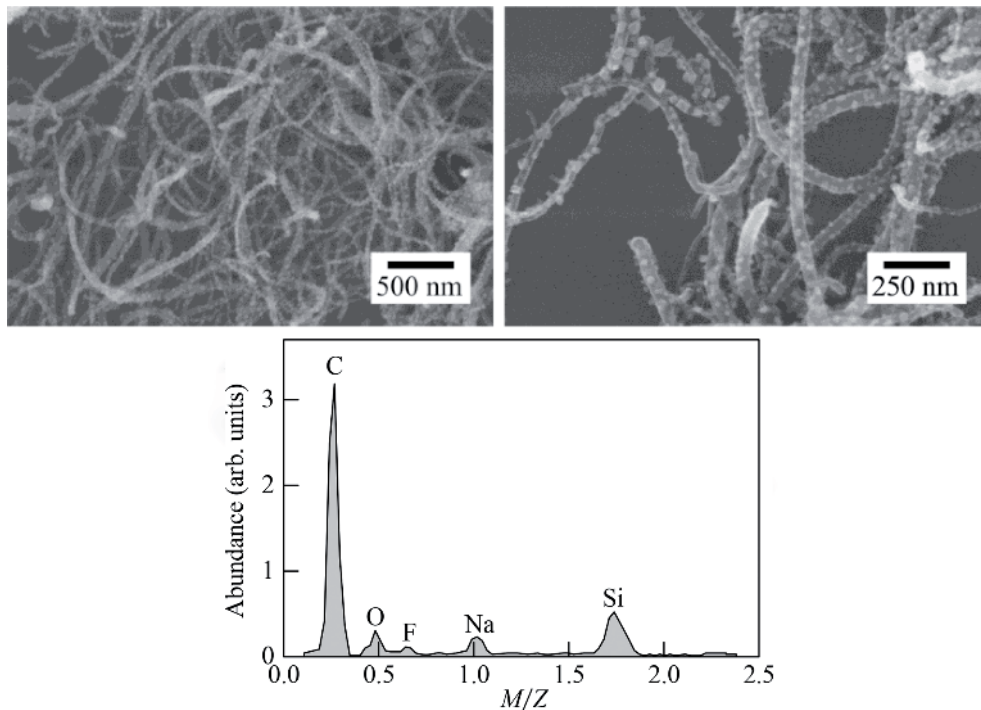


Figure 14. Nanocrystals of NaF formed on the surface of oxidized MWCNT (top panel). Mass spectrum of NaF nanocrystals “decorated” MWCNTs (bottom panel); M/Z is the ratio of ion mass to its charge.

6. Carbon nanotube assembling and physical cross-linking

We have developed a novel physical method of stable linkage between neighboring carbon nanotubes in 2D layers (dense arrays), by intertube bridging using Ar^+ -ion beam (**Figure 15**).

The carbon nanotube layer has modified using ion beam irradiation. It introduces stable link formation between neighboring carbon nanotubes, in other words, bridging or physical cross-linking.

The intertube bridging (cross-linking) of MWCNTs and SWCNTs in the arrays was observed under the Ar^+ -ion irradiation. This method can be utilized for the improvement of the electrical and thermal conductivity properties of carbon nanotube layers for electron transport heat transfer applications.

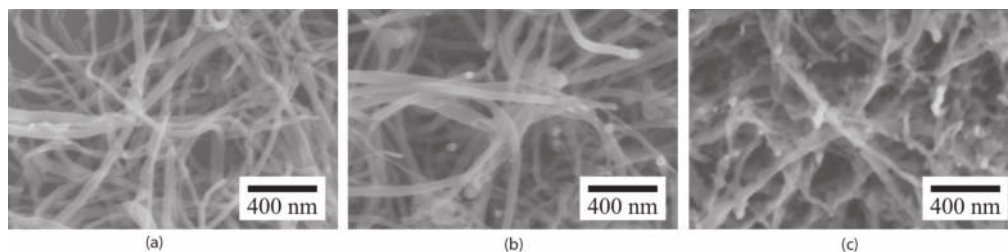


Figure 15. (a) The image of the initial (unprocessed) array of multiwall carbon nanotubes. (b) The image of a “short-time” processing regime: 6 kV, 60 s. Just the ends of the tubes attacked by Ar^+ -ion irradiation. (c) The image of a “long-time” processing regime: 6 kV, 10 min. The continuous cross-linked network of the MW carbon after the Ar^+ -ion irradiation is observed.

7. Nanosensor applications of carbon nanotube films

In this chapter we would like to point out an example of application of films of MWCNT as a new icing condition resistive sensor that we have developed. These sensors are based on the adsorption of a molecular thin layer of water on the surface of carbon nanotubes and on the detection of the first-order phase transition of water molecules into ice. This transition is very well detected as a result of non-monotonous dependence of the resistance of the sensor vs. temperature in the vicinity of the freezing point due to a virtual “field effect transistor.” Electronic transport in carbon nanotube films, assembled into the resistive films, was found to be extremely sensitive to the adsorption of polar H₂O molecules.

Modern sensors of icing conditions (optical or piezo devices) are based on the detection of the actual (significantly thick) layers of ice formed on the surfaces. The accumulation of the ice layer is a fast process, and detection of the massive ice formation is too late for the safety of the aircrafts.

We have developed a method of assembling MWCNT films of arbitrary thickness for sensor applications. This method involves oxidation of carbon nanotubes and does have several major advantages over the conventional methods of carbon nanotube assembling via their functionalization. The assembled carbon nanotube films are dense, homogeneous, and strong on the macro level, but internally they consist of disordered structure of self-assembled carbon nanotubes, forming conductive medium, as it is seen in **Figure 16**. Besides they are hydrophilic and adsorb water molecules strongly. Based on our experience of multiwall CNT characterization [22, 74], we were able to study them at fixed values of humidity and temperature variation.

Standard sensors of relative humidity based on multiwall carbon nanotubes were developed earlier [75, 76].

We have found that the adsorption of the water vapor at the temperatures close to freezing conditions generates a specific non-monotonous dependence of the resistance of the sensor vs. temperature.

The intensive precipitation of the water vapor, when the temperature is decreasing, results in the increase of the resistance of the nanosensor, due to the “field effect” created by the adsorbed polar water molecules on the surface of slightly charged CNT tubes. A further decrease of the temperature passing the freezing point results in the sudden drop of the resistance (“lambda-point”-type curve at the phase transitions of the first order) (see the insert in **Figure 17**) due to the water transition to nonpolar ice crystal. As a result, the “field effect” disappears, and the resistance of the carbon nanotubes decreases again.

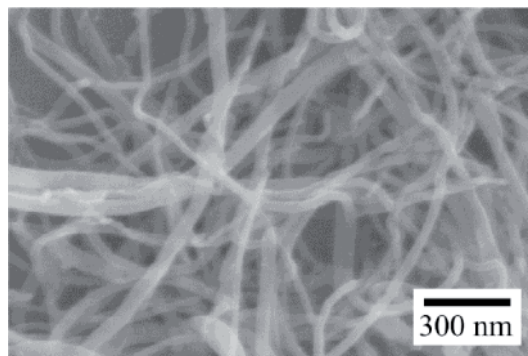


Figure 16.
SEM image of the morphology of multiwall carbon nanotube film.

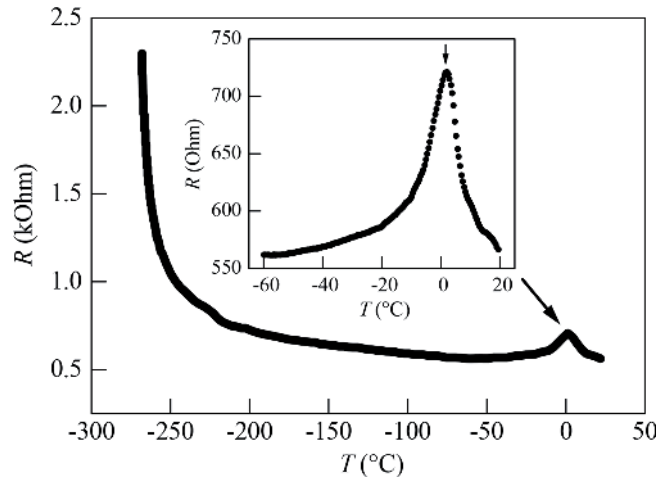


Figure 17. Temperature dependence of the resistance of the MWCNT layer in the presence of water vapors. Note, the maximum of the resistance was found to be located in the nearest proximity of the water freezing point at $T = 0^{\circ}\text{C}$.

In order to verify, if the positions of the peaks correspond to the humidity (dew point or frost point), we did temperature scans at different controllable values of the humidity. The dependences of the resistance of the CNT sensor measured at fast temperature scan at different humidity levels and temperature variations from approx $+50^{\circ}\text{C}$ down to -50°C are plotted in **Figure 18**. The temperature dependences of the resistance of the CNT sensors measured at the slow temperature scan ($\leq 0.01^{\circ}\text{C}/\text{s}$ in the cryo-cell of our own design) are shown in **Figure 19**. As can be seen in **Figures 18** and **19**, if the temperature drops down, a significant resistance increase takes place, followed by the maximum point of the resistance and sudden resistance drop due to the ice formation.

There is a significant difference in the observation of the dew points and the frost points using CNT sensors. If we observe T_{dew} , which is higher than the freezing point, we observe significant resistance increase due to condensation. Then the saturation occurs and, at the freezing point, is characterized by a sudden resistance decrease. In the meantime, if we observe frost points instead, while the temperature decreases, the condensation corresponds to the frost point.

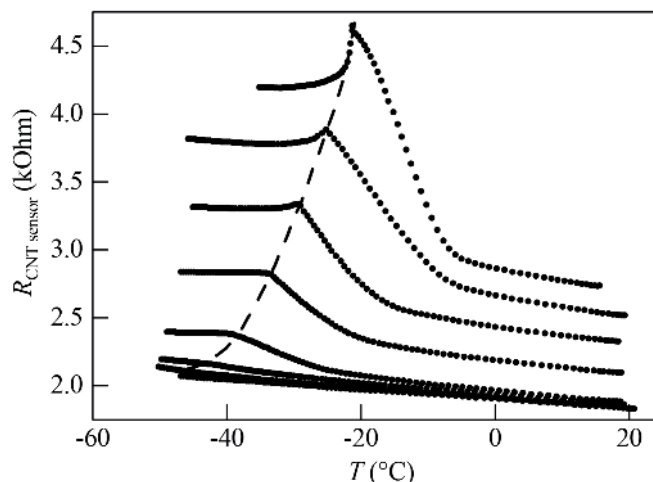


Figure 18. The resistance of the CNT sensor vs. temperature at different humidity levels at the fast temperature scan of $\sim 1^{\circ}\text{C}/\text{s}$.

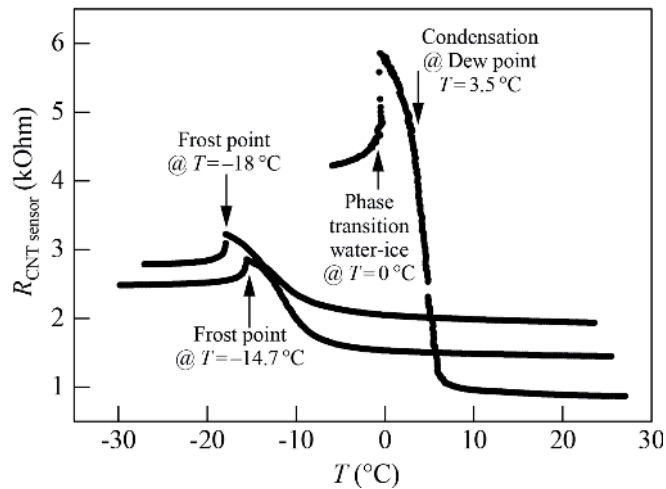


Figure 19. Temperature dependences of the resistance of the CNT sensors measured at the slow temperature scan $\leq 0.01^\circ\text{C/s}$ in the cryo-cell of our own design.

8. Coating carbon nanotubes with diamond-like carbon films

A commercial plasma CVD setup was used to deposit a diamond-like carbon (DLC) film over the CNT matrix (**Figure 20**).

We found out that thin (~ 50 nm thick) DLC films have significantly improved mechanical properties.

DLC coating on the CNT layers has a high degree of wettability. We also determined that it is adding significant reinforcement to the MWCNT matrix.

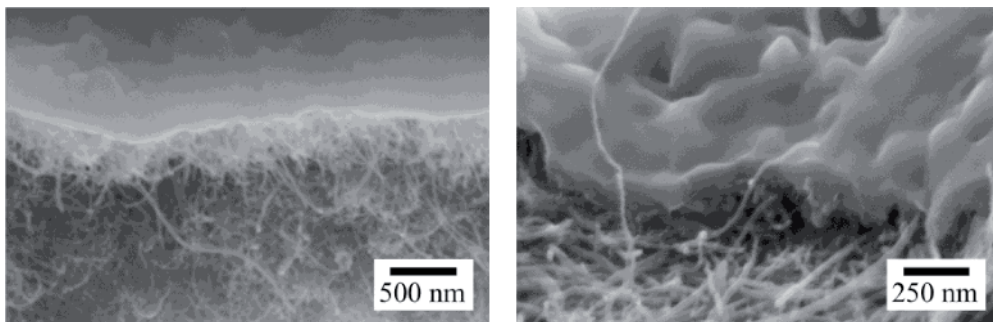


Figure 20. SEM pictures of the DLC film deposited on the top of the MWCNT layer.

9. Conclusions

Several methods of assembling MWCNTs into monolayers and freestanding films of arbitrary thickness have been developed.

We have studied assemblies of pristine (non-modified) CNTs, CNTs modified by organic chemical functionalization, and the oxidized CNTs.

We have experimentally tested the electrical transport properties of assembled layers (films) of non-functionalized, functionalized, and oxidized MWCNTs.

The temperature dependence of the resistance and magnetoresistance of the self-assembled arrays of MWCNT, tested in the wide temperature range, were considered as a tool to determine the transport characteristics of the films, important for further applications.

The negative magnetoresistance as a characteristic of weak localization state was observed. In addition to the negative magnetoresistance at high fields for functionalized nanotubes, we observed positive magnetoresistance at low fields.

The layers of MWCNTs have been considered as attractive materials for various nanosensors and as the electrodes of electrochemical energy storage devices. We have shown an example of application of films of MWCNT as an icing condition resistive sensor. A very strong catalytic activity of an outer surface of MWCNT, modified by oxidation, has been pointed out as well.

We have developed a novel method of stable physical linkage between the neighboring carbon nanotubes in 2D layers (dense arrays) by intertube bridging using Ar⁺-ion beam and the method of MWCNT coating with diamond-like carbon films as well.

Acknowledgements

V.S. is very grateful to the Ministry of Education of France for the fellowship, the National Science Foundation of Switzerland, Award #7BYPJ065694 for support, the Laboratoire National des Champs Magnetiques Intenses de Toulouse, Dr. Jean Galibert and Prof. Laszlo Forró for hospitality. He would like to express his sincere gratitude to Dr. J. Quinn for the help with SEM imaging, Dr. M. Seo for the help with TEM, Dr. Y. Seo and Dr. J. Koo for the help with MWCNT oxidation, and Dr. V. Zaitsev for the help with the organic functionalization of MWCNT. Finally, V.S. acknowledges support of the Sensor CAT and the Research Foundation of SUNY. N.P. acknowledges support of the Belarusian Research Program “Convergence-2020” and the Belarusian Republican Foundation for Fundamental Research (Grant No. F18R-253).

Author details

Vladimir Samuilov^{1,2*}, Jean Galibert² and Nikolai Poklonski³


1 Department of Materials Science, SUNY at SB, Stony Brook, NY, USA

2 Laboratoire National des Champs Magnetiques Intenses, LNCMI-EMFL, CNRS/INSA/UGA/UPS, Toulouse and Grenoble, France

3 Department of Physics, Belarusian State University, Minsk, Belarus

*Address all correspondence to: vladimir.samuilov@stonybrook.edu

IntechOpen

© 2019 The Author(s). Licensee IntechOpen. This chapter is distributed under the terms of the Creative Commons Attribution License (<http://creativecommons.org/licenses/by/3.0>), which permits unrestricted use, distribution, and reproduction in any medium, provided the original work is properly cited. 

References

- [1] Iijima S. Helical microtubules of graphitic carbon. *Nature*. 1991;**354**:56-58. DOI: 10.1038/354056a0
- [2] Dai H. Carbon nanotubes: Opportunities and challenges. *Surface Science*. 2002;**500**:218-241. DOI: 10.1016/S0039-6028(01)01558-8
- [3] Forró L, Schönenberger C. Physical properties of multi-wall nanotubes. In: Dresselhaus MS, Dresselhaus G, Avouris P, editors. *Carbon Nanotubes, Topics Applied Physics*. Vol. 80. Berlin: Springer; 2001. pp. 329-391. DOI: 10.1007/3-540-39947-X_13
- [4] Poklonski NA, Vyrko SA, Siahlo AI, Poklonskaya ON, Ratkevich SV, Hieu NN, et al. Synergy of physical properties of low-dimensional carbon-based systems for nanoscale device design. *Materials Research Express*. 2019;**6**:042002. DOI: 10.1088/2053-1591/aafb1c
- [5] Avouris P. Carbon nanotube electronics. *Chemical Physics*. 2002;**281**:429-445. DOI: 10.1016/S0301-0104(02)00376-2
- [6] Hartmann RR, Kono J, Portnoi ME. Terahertz science and technology of carbon nanomaterials. *Nanotechnology*. 2014;**25**:322001. DOI: 10.1088/0957-4484/25/32/322001
- [7] Martel R, Schmidt T, Shea HR, Hertel T, Avouris P. Single- and multi-wall carbon nanotube field-effect transistors. *Applied Physics Letters*. 1998;**73**:2447-2449. DOI: 10.1063/1.122477
- [8] Tans SJ, Verschueren ARM, Dekker C. Room-temperature transistor based on a single carbon nanotube. *Nature*. 1998;**393**:49-52. DOI: 10.1038/29954
- [9] Martel R, Derycke V, Lavoie C, Appenzeller J, Chan KK, Tersoff J, et al. Ambipolar electrical transport in semiconducting single-wall carbon nanotubes. *Physical Review Letters*. 2001;**87**:256805. DOI: 10.1103/PhysRevLett.87.256805
- [10] Goze C, Vaccarini L, Henrard L, Bernier P, Hernandez E, Rubio A. Elastic and mechanical properties of carbon nanotubes. *Synthetic Metals*. 1999;**103**:2500-2501. DOI: 10.1016/S0379-6779(98)01071-6
- [11] Fraysse J, Minett AI, Jaschinski O, Duesberg GS, Roth S. Carbon nanotubes acting like actuators. *Carbon*. 2002;**40**:1735-1739. DOI: 10.1016/S0008-6223(02)00041-6
- [12] Vigolo B, Pénicaud A, Coulon C, Sauder C, Pailler R, Journet C, et al. Macroscopic fibers and ribbons of oriented carbon nanotubes. *Science*. 2000;**290**:1331-1334. DOI: 10.1126/science.290.5495.1331
- [13] Frackowiak E, Gautier S, Gaucher H, Bonnamy S, Beguin F. Electrochemical storage of lithium multiwalled carbon nanotubes. *Carbon*. 1999;**37**:61-69. DOI: 10.1016/S0008-6223(98)00187-0
- [14] Collins PG, Bradley K, Ishigami M, Zettl A. Extreme oxygen sensitivity of electronic properties of carbon nanotubes. *Science*. 2000;**287**:1801-1804. DOI: 10.1126/science.287.5459.1801
- [15] Varghese OK, Kichambre PD, Gong D, Ong KG, Dickey EC, Grimes CA. Gas sensing characteristics of multi-wall carbon nanotubes. *Sensors and Actuators B: Chemical*. 2001;**81**:32-41. DOI: 10.1016/S0925-4005(01)00923-6
- [16] Kong J, Franklin NR, Zhou C, Chaplin MG, Peng S, Cho K, et al. Nanotube molecular wires as chemical sensors. *Science*. 2000;**287**:622-625. DOI: 10.1126/science.287.5453.622

- [17] Guo Z, Sadler PJ, Tsang SC. Immobilization and visualization of DNA and proteins on carbon nanotubes. *Advanced Materials*. 1998;**10**:701-703. DOI: 10.1002/(SICI)1521-4095(199806)10:9<701::AID-ADMA701>3.0.CO;2-4
- [18] Davis JJ, Green MLH, Hill HAO, Leung YC, Sadler PJ, Sloan J, et al. The immobilization of proteins in carbon nanotubes. *Inorganica Chimica Acta*. 1998;**272**:261-266. DOI: 10.1016/S0020-1693(97)05926-4
- [19] Balavoine F, Schultz P, Richard C, Mallouh V, Ebbesen TW, Mioskowski C. Helical crystallization of proteins on carbon nanotubes: A first step towards the developments of new biosensors. *Angewandte Chemie, International Edition*. 1999;**38**:1912-1915. DOI: 10.1002/(SICI)1521-3773(19990712)38:13/14<1912::AID-ANIE1912>3.0.CO;2-2
- [20] Chen RJ, Zhang Y, Wang D, Dai H. Noncovalent sidewall functionalization of single-walled carbon nanotubes for protein immobilization. *Journal of the American Chemical Society*. 2001;**123**:3838-3839. DOI: 10.1021/ja010172b
- [21] Xue HG, Sun WL, He BJ, Shen ZQ. A new application of carbon nanotubes constructing biosensor. *Chinese Chemical Letters*. 2002;**13**:799-800
- [22] Ksenevich V, Galibert J, Samuilov V. Charge transport in carbon nanotube films and fibers. In: Marulanda JM, editor. *Carbon Nanotubes*. Rijeka, Croatia: InTech; 2010. pp. 123-146. DOI: 10.5772/39422
- [23] Ksenevich VK, Gorbachuk NI, Poklonski NA, Samuilov VA, Kozlov ME, Wieck AD. Impedance of single-walled carbon nanotube fibers. *Fullerenes, Nanotubes, and Carbon Nanostructures*. 2012;**20**:434-438. DOI: 10.1080/1536383X.2012.655562
- [24] Frank S, Poncharal P, Wang ZL, de Heer WA. Carbon nanotube quantum resistors. *Science*. 1998;**280**:1744-1746. DOI: 10.1126/science.280.5370.1744
- [25] Bockrath M, Cobden DH, Lu J, Rinzler AG, Smalley RE, Balents L, et al. Luttinger-liquid behaviour in carbon nanotubes. *Nature*. 1999;**397**:598-601. DOI: 10.1038/17569
- [26] Nygard J, Cobden DH, Bockrath M, McEuen PL, Lindelof PE. Electrical transport measurements on single-walled carbon nanotubes. *Applied Physics A: Materials Science & Processing*. 1999;**69**:297-304. DOI: 10.1007/s003390051
- [27] Zhou C, Kong J, Dai H. Electrical measurements of individual semiconducting single-walled carbon nanotubes of various diameter. *Applied Physics Letters*. 2000;**76**:1597-1599. DOI: 10.1063/1.126107
- [28] Shea HR, Martel R, Avouris P. Electrical transport in rings of single-wall nanotubes: One-dimensional localization. *Physical Review Letters*. 2000;**84**:4441-4444. DOI: 10.1103/PhysRevLett.84.4441
- [29] Laird EA, Kuemmeth F, Steele GA, Grove-Rasmussen K, Nygård J, Flensberg K, et al. Quantum transport in carbon nanotubes. *Reviews of Modern Physics*. 2015;**87**:703-764. DOI: 10.1103/RevModPhys.87.703
- [30] Langer L, Bayot V, Grivei E, Issi J-P, Heremans JP, Olk CH, et al. Quantum transport in a multiwalled carbon nanotube. *Physical Review Letters*. 1996;**76**:479-482. DOI: 10.1103/PhysRevLett.76.479
- [31] Bachtold A, Henny M, Terrier C, Strunk C, Schönenberger C, Salvetat J-P, et al. Contacting carbon nanotubes selectively with low-ohmic contacts four-probe electric measurement.

- Applied Physics Letters. 1998;**73**:274-276. DOI: 10.1063/1.121778
- [32] Bachtold A, Strunk C, Salvetat J-P, Bonard J-M, Forró L, Nussbaumer T, et al. Aharonov–Bohm oscillations in carbon nanotubes. *Nature*. 1999;**397**:673–675. DOI: 10.1038/17755
- [33] Schönenberger C, Bachtold A, Strunk C, Salvetat J-P, Forró L. Interference and interaction in multi-wall carbon nanotubes. *Applied Physics A: Materials Science & Processing*. 1999;**69**:283–295. DOI: 10.1007/s003390051
- [34] Lee J-O, Kim J-R, Kim J-J, Kim JH, Kim N, Park JW, et al. Magnetoresistance and differential conductance in multiwalled carbon nanotubes. *Physical Review B*. 2000;**61**:R16362–R16365. DOI: 10.1103/PhysRevB.61.R16362
- [35] Liu K, Avouris P, Martel R, Hsu WK. Electrical transport in doped multiwalled carbon nanotubes. *Physical Review B*. 2001;**63**:161404. DOI: 10.1103/PhysRevB.63.161404
- [36] Stojetz B, Miko C, Forró L, Strunk C. Effect of band structure on quantum interference in multiwall carbon nanotubes. *Physical Review Letters*. 2005;**94**:186802. DOI: 10.1103/PhysRevLett.94.186802
- [37] Ishikawa S, Enomoto R, Aoki N, Umishita K, Ishibashi K, Aoyagi Y, et al. One-dimensional conduction in multi-wall carbon nano-tubes. *Springer Proceedings in Physics*. 2001;**87**:1661–1662
- [38] Liu K, Roth S, Duesberg G, Wagenhals M, Journet C, Bernier P. Transport properties of single-walled carbon nanotubes. *Synthetic Metals*. 1999;**103**:2513–2514. DOI: 10.1016/S0379-6779(98)01081-9
- [39] Eletsii AV, Knizhnik AA, Potapkin BV, Kenny JM. Electrical characteristics of carbon nanotube doped composites. *Physics-Uspekhi*. 2015;**58**:209–251. DOI: 10.3367/UFNe.0185.201503a.0225
- [40] Stahl H, Appenzeller J, Martel R, Avouris P, Lengeler B. Intertube coupling in ropes of single-wall carbon nanotubes. *Physical Review Letters*. 2000;**85**:5186–5189
- [41] Krstić V, Roth S, Burghard M. Phase breaking in three-terminal contacted single-walled carbon nanotube bundles. *Physical Review B*. 2000;**62**:R16352–R16355. DOI: 10.1103/PhysRevB.62.R16353
- [42] Park JG, Kim GT, Park JH, Yu HY, McIntosh G, Krstic V, et al. Quantum transport in low-dimensional organic nanostructures. *Thin Solid Films*. 2001;**393**:161–167. DOI: 10.1016/S0040-6090(01)01064-1
- [43] Fischer JE, Dai H, Thess A, Lee R, Hanjani NM, Dehaas DL, et al. Metallic resistivity in crystalline ropes of single-wall carbon nanotubes. *Physical Review B*. 1997;**55**:R4921–R4924. DOI: 10.1103/PhysRevB.55.R4921
- [44] Kaiser AB, Park YW, Kim GT, Choi ES, Düsberg G, Roth S. Electronic transport in carbon nanotube ropes and mats. *Synthetic Metals*. 1999;**103**:2547–2550. DOI: 10.1016/S0379-6779(98)00222-7
- [45] Kaiser AB, Düsberg G, Roth S. Heterogeneous model for conduction in carbon nanotubes. *Physical Review B*. 1998;**57**:1418–1421. DOI: 10.1103/PhysRevB.57.1418
- [46] Kim GT, Jhang SH, Park JG, Park YW, Roth S. Non-ohmic current–voltage characteristics in single-wall carbon nanotube network. *Synthetic Metals*. 2001;**117**:123–126. DOI: 10.1016/S0379-6779(00)00551-8

- [47] Franklin NR, Dai H. An enhanced CVD approach to extensive nanotube networks with directionality. *Advanced Materials*. 2000;**12**:890-894. DOI: 10.1002/1521-4095(200006)12:12<890:AID-ADMA890>3.0.CO;2-K
- [48] Baumgartner G, Carrard M, Zuppiroli L, Bacsa W, de Heer WA, Forró L. Hall effect and magnetoresistance of carbon nanotube films. *Physical Review B*. 1997;**55**:6704-6707. DOI: 10.1103/PhysRevB.55.6704
- [49] Ausman KD, Piner R, Lurie O, Ruoff RS, Korobov M. Organic solvent dispersions of single-walled carbon nanotubes: Toward solutions of pristine nanotubes. *The Journal of Physical Chemistry B*. 2000;**104**:8911-8915. DOI: 10.1021/jp002555m
- [50] Krstic V, Muster J, Duesberg GS, Philipp G, Burghard M, Roth S. Electrical transport in single-walled carbon nanotube bundles embedded in Langmuir–Blodgett monolayers. *Synthetic Metals*. 2000;**110**:245-249. DOI: 10.1016/S0379-6779(99)00302-1
- [51] Krstic V, Duesberg GS, Muster J, Burghard M, Roth S. Langmuir–Blodgett films of matrix-diluted single-walled carbon nanotubes. *Chemistry of Materials*. 1998;**10**:2338-2340. DOI: 10.1021/cm980207f
- [52] Burghard M, Krstic V, Duesberg GS, Philipp G, Muster J, Roth S. Carbon SWNTs as wires and structural templates between nanoelectrodes. *Synthetic Metals*. 1999;**103**:2540-2542. DOI: 10.1016/S0379-6779(99)80005-8
- [53] Sano M, Kamino A, Okamura J, Shinkai S. Self-organization of PEO-*graft*-single-walled carbon nanotubes in solutions and Langmuir–Blodgett films. *Langmuir*. 2001;**17**:5125-5128. DOI: 10.1021/la010126p
- [54] Holzinger M, Vostrovsky O, Hirsch A, Hennrich F, Kappes M, Weiss R, et al. Sidewall functionalization of carbon nanotubes. *Angewandte Chemie, International Edition*. 2001;**40**:4002-4005. DOI: 10.1002/1521-3773(20011105)40:21<4002:AID-ANIE4002>3.0.CO;2-8
- [55] Hirsch A. Functionalization of single-walled carbon nanotubes. *Angewandte Chemie, International Edition*. 2002;**41**:1853-1859. DOI: 10.1002/1521-3773(20020603)41:11<1853::AID-ANIE1853>3.0.CO;2-N
- [56] Huang W, Lin Y, Taylor S, Gaillard J, Rao AM, Sun Y-P. Sonication-assisted functionalization and solubilization of carbon nanotubes. *Nano Letters*. 2002;**2**:231-234
- [57] Berger C, Song Z, Li X, Wu X, Brown N, Maud D, et al. Magnetotransport in high mobility epitaxial graphene. *Physica Status Solidi A: Applications and Materials Science*. 2007;**204**:1746-1750. DOI: 10.1002/pssa.200675352
- [58] Sharapov SG, Gusynin VP, Beck H. Magnetic oscillations in planar systems with the Dirac-like spectrum of quasiparticle excitations. *Physical Review B*. 2004;**69**:075104. DOI: 10.1103/PhysRevB.69.075104
- [59] Berger C, Song Z, Li X, Wu X, Brown N, Naud C, et al. Electronic confinement and coherence in patterned epitaxial graphene. *Science*. 2006;**312**:1191-1196. DOI: 10.1126/science.1125925
- [60] Kawabata A. Theory of negative magnetoresistance in three-dimensional systems. *Solid State Communications*. 1980;**34**:431-432. DOI: 10.1016/0038-1098(80)90644-4
- [61] Ousset JC, Rakoto H, Broto JM, Dupuis VV, Askenazy S, Durand J, et al. Weak-localization effects in $V_{1-x}Si_x$ amorphous alloys with high Si content.

- Physical Review B. 1987;**36**:5432-5436.
DOI: 10.1103/PhysRevB.36.5432
- [62] Ulmet JP, Bachère L, Askenazy S, Ousset JC. Negative magnetoresistance in some dimethyltrimethylene-tetraselenafulvalenium salts: A signature of weak localization effects. *Physical Review B*. 1988;**38**:7782-7788. DOI: 10.1103/PhysRevB.38.7782
- [63] Nguyen VI, Spivak BZ, Shklovskii BI. Tunnel hopping in disordered systems. *Journal of Experimental and Theoretical Physics*. 1985;**62**:1021-1029
- [64] Sivan U, Entin-Wohlman O, Imry Y. Orbital magnetoconductance in the variable-range-hopping regime. *Physical Review Letters*. 1988;**60**:1566-1569. DOI: 10.1103/PhysRevLett.60.1566
- [65] Sheng P. Fluctuation-induced tunneling conduction in disordered materials. *Physical Review B*. 1980;**21**:2180-2195. DOI: 10.1103/PhysRevB.21.2180
- [66] Yasawa K. Negative magnetoresistance in pyrolytic carbons. *Journal of the Physical Society of Japan*. 1969;**26**:1407-1419. DOI: 10.1143/JPSJ.26.1407
- [67] Bahr JL, Tour JM. Covalent chemistry of single-wall carbon nanotubes. *Journal of Materials Chemistry*. 2002;**12**:1952-1958. DOI: 10.1039/B201013P
- [68] Chiu PW, Duesberg GS, Dettlaff-Weglikowska U, Roth S. Interconnection of carbon nanotubes by chemical functionalization. *Applied Physics Letters*. 2002;**80**:3811-3813. DOI: 10.1063/1.1480487
- [69] Georgakilas V, Kordatos K, Prato M, Guldi DM, Holzinger M, Hirsch A. Organic functionalization of carbon nanotubes. *Journal of the American Chemical Society*. 2002;**124**:760-761. DOI: 10.1021/ja016954m
- [70] Dresselhaus PD, Papavassiliou CM, Wheeler RG, Sacks RN. Observation of spin precession in GaAs inversion layers using antilocalization. *Physical Review Letters*. 1992;**68**:106-109. DOI: 10.1103/PhysRevLett.68.106
- [71] Chen GL, Han J, Huang TT, Datta S, Janes DB. Observation of the interfacial-field-induced weak antilocalization in InAs quantum structures. *Physical Review B*. 1993;**47**:4084-4087. DOI: 10.1103/PhysRevB.47.4084
- [72] Fujimoto A, Kobori H, Ohyama T, Ishida S, Satoh K, Kusaka T, et al. Comparison of magnetoconductance of the δ -doped layer and bulk crystal of Si:Sb in the weak localization regime. *Physica B: Condensed Matter*. 2001;**302-303**:7-11. DOI: 10.1016/S0921-4526(01)00399-4
- [73] Liu K, Roth S, Düsberg GS, Kim GT, Popa D, Mukhopadhyay K, et al. Antilocalization in multiwalled carbon nanotubes. *Physical Review B*. 2000;**61**:2375-2379. DOI: 10.1103/PhysRevB.61.2375
- [74] Wang G, Tan Z, Liu X, Chawda S, Koo J-S, Samuilov V, et al. Conducting MWNT/poly(vinyl acetate) composite nanofibres by electrospinning. *Nanotechnology*. 2006;**17**:5829-5835. DOI: 10.1088/0957-4484/17/23/019
- [75] Chen W-P, Zhao Z-G, Liu X-W, Zhang Z-X, Suo C-G. A capacitive humidity sensor based on multi-wall carbon nanotubes (MWCNTs). *Sensors*. 2009;**9**:7431-7444. DOI: 10.3390/s90907431
- [76] Lee C-Y, Lee G-B. Humidity sensors: A review. *Sensor Letters*. 2005;**3**:1-14. DOI: 10.1166/sl.2005.001